THE JOURNAL OF BIOLOGICAL CHEMISTRY VOL. 284, NO. 9, pp. 5859–5868, February 27, 2009

Methylalpinumisoflavone Inhibits Hypoxia-inducible Factor-1 (HIF-1) Activation by Simultaneously Targeting Multiple Pathways*[S]

Received for publication, September 2, 2008, and in revised form, December 1, 2008 Published, JBC Papers in Press, December 17, 2008, DOI 10.1074/jbc.M806744200

Yang Liu[‡], Coothan K. Veena[‡], J. Brian Morgan[‡], Kaleem A. Mohammed[‡], Mika B. Jekabsons[§], Dale G. Nagle[‡¶1], and Yu-Dong Zhou[‡2]

From the [‡]Department of Pharmacognosy and [¶]Research Institute of Pharmaceutical Sciences, School of Pharmacy, and [§]Department of Biology, University of Mississippi, University, Mississippi 38677

Hypoxia is a common feature of solid tumors, and the extent of tumor hypoxia correlates with advanced disease stages and treatment resistance. The transcription factor hypoxia-inducible factor-1 (HIF-1) represents an important tumor-selective molecular target for anticancer drug discovery directed at tumor hypoxia. A natural product chemistry-based approach was employed to discover small molecule inhibitors of HIF-1. Bioassay-guided isolation of an active lipid extract of the tropical legumaceous plant *Lonchocarpus glabrescens* and structure elucidation afforded two new HIF-1 inhibitors: alpinumisoflavone (compound 1) and 4′-*O*-methylalpinumisoflavone (compound 2). In human breast tumor T47D cells, compounds 1 and 2 inhibited hypoxia-induced HIF-1 activation with IC_{50} values of 5 and 0.6 μM, respectively. At the concentrations that inhibited HIF-1 activation, compound 2 inhibited hypoxic induction of HIF-1 target genes (*CDKN1A*, *GLUT-1*, and *VEGF*), tumor angiogenesis *in vitro*, cell migration, and chemotaxis. Compound 2 inhibits HIF-1 activation by blocking the induction of nuclear HIF-1α protein, the oxygen-regulated subunit that controls HIF-1 activity. Mechanistic studies indicate that, unlike rotenone and other mitochondrial inhibitors, compound 2 represents the first small molecule that inhibits HIF-1 activation by simultaneously suppressing mitochondrial respiration and disrupting protein translation *in vitro*. This unique mechanism distinguishes compound 2 from other small molecule HIF-1 inhibitors that are simple mitochondrial inhibitors or flavanoid-based protein kinase inhibitors.

Hypoxia (reduced oxygen tension) arises when the existing tumor blood vessels fail to meet the oxygen demand of the rapidly growing tumor cells. To compensate for this decrease in oxygen supply, hypoxic tumor cells activate the expression of genes that range in function from those that promote anaerobic metabolism to those that initiate tumor angiogenesis (1–3). Newly formed tumor blood vessels often fail to fully mature. This leads to sluggish and irregular blood flow. As a result, certain regions of tumors are under constant hypoxic stress (3, 4). Hypoxic tumor cells that have adapted to an environment low in oxygen and nutrients are more aggressive and resistant to treatment (5). In clinical settings, the extent of tumor hypoxia correlates with advanced disease stages, poor prognosis, and treatment resistance (3). Currently, there is no approved drug that specifically targets hypoxic tumor cells. It is clear that tumor hypoxia is an important unmet therapeutic need and deserves considerable drug discovery efforts.

One major molecular target for hypoxia-selective anticancer drug discovery is the transcription factor HIF-1.[3] Semenza and Wang (6) first described HIF-1 as the transcriptional activator responsible for the hypoxic induction of erythropoietin. Functioning as a key regulator of oxygen homeostasis, HIF-1 is a heterodimer of the basic helix-loop-helix PER-ARNT-Sim proteins HIF-1α and HIF-1β/ARNT (7). In general, HIF-1α protein is degraded rapidly under normoxic conditions by the ubiquitin-proteasome pathway and is stabilized under hypoxic conditions, whereas HIF-1β protein is constitutively expressed (8). Upon activation, HIF-1 binds to the hypoxia-response element in the promoters of target genes and activates transcription. The classical oxygen-dependent post-translational regulation of HIF-1α protein includes prolyl hydroxylation-dependent proteasome degradation and asparaginyl hydroxylation-associated inactivation (9–11). Recent studies have implicated other oxygen-independent pathways that regulate HIF-1α protein degradation (12, 13). Over sixteen years of research has revealed the important role in cancer biology that HIF-1 plays by regulating the expression of genes involved in processes such as immortalization, genetic instability, dedifferentiation and stem cell maintenance, tumor angiogenesis, metabolic reprogramming, survival and resistance to apoptosis, migration/in-

* This work was supported, in whole or in part, by National Institutes of Health Grants CA98787 and P20RR021929 and conducted in a facility constructed with National Institutes of Health Research Facilities Improvement Grant C06 RR-14503-01. This work was also supported by National Oceanic and Atmospheric Administration/National Institute of Undersea Science and Technology Grant NA16RU1496. The costs of publication of this article were defrayed in part by the payment of page charges. This article must therefore be hereby marked "*advertisement*" in accordance with 18 U.S.C. Section 1734 solely to indicate this fact.

[S] The on-line version of this article (available at http://www.jbc.org) contains supplemental Fig. S1.

[1] To whom correspondence may be addressed. Tel.: 662-915-7143; Fax: 662-915-6975; E-mail: dnagle@olemiss.edu.

[2] To whom correspondence may be addressed. Tel.: 662-915-2012; Fax: 662-915-6975; E-mail: ydzhou@olemiss.edu.

[3] The abbreviations used are: HIF-1, hypoxia-inducible factor-1; ETC, electron transport chain; HUVEC, human umbilical vein endothelial cell; MIC, minimum inhibitory concentration; ROS, reactive oxygen species; VEGF, vascular endothelial growth factor; ELISA, enzyme-linked immunosorbent assay; DMEM, Dulbecco's modified Eagle's medium; ANOVA, analysis of variance; FBS, fetal bovine serum; MTT, methylthiazoyldiphenyltetrazolium bromide.

vasion and metastasis, and treatment resistance (14, 15). In general, HIF-1 activation promotes hypoxic adaptation and survival by increasing oxygen delivery, decreasing oxygen consumption, expressing growth factors for autocrine signaling, suppressing cell death, and promoting metastasis (14, 15). Clinical studies indicate that HIF-1α protein expression correlates with advanced disease stages, metastasis, treatment resistance, and poor prognosis in cancer patients (16–18). In animal models, HIF-1 inhibition reduced tumor vascularity and retarded tumor growth (19, 20). When HIF-1 inhibition was combined with chemotherapy or radiation, enhanced treatment outcomes were observed in preclinical models (21, 22). Thus, small molecule HIF-1 inhibitors represent potential drug leads that will suppress tumor growth and enhance chemotherapy/radiation by inhibiting hypoxia-induced gene expression.

Most laboratories use a pure compound library-based screening approach for the discovery of small molecule HIF-1 inhibitors. Representative HIF-1 inhibitors discovered include the following: topotecan, which is an approved drug (23); echinomycin, which is in clinical trial (24); chetomin (20), a weakly active benzopyran derivative 103D5R (25), emetine and analogs of emetine and actinomycin D (26, 27), and a pyrroloquinoline derivative DJ12 (28). Most of these compounds have a narrow window between HIF-1 inhibitory activity and cytotoxicity. In addition to these HIF-1 inhibitors identified through screening efforts, a number of anticancer agents have also been shown to suppress HIF-1 activation (15). Using a natural product chemistry-based approach, we have discovered chemically diverse HIF-1 inhibitors such as manassantins that function at nanomolar concentrations with a wide window between their HIF-1 inhibitory activity and cytotoxicity (29, 30). This study describes the discovery and characterization of HIF-1 inhibitors from the plant *Lonchocarpus glabrescens*.

EXPERIMENTAL PROCEDURES

Plant Material, Extraction, and Isolation—The plant material (*L. glabrescens*) was collected by Dr. Sidney McDaniel from Punchana, Peru, on August 8, 1991. Voucher specimen (IBE 31253) is stored at the National Center for Natural Products Research repository, University of Mississippi, University, MS. Powdered plant material (NP 9179) was extracted with ethanol. Chromatographic separation of the active extract and isolation of the active compounds were performed using standard methods. The NMR spectra of **1–3** match those previously published (31).

Cell Culture and Cell-based Reporter Assay—Human breast tumor T47D and MDA-MB-231, prostate tumor PC-3, and DU-145 cell lines (ATCC) were maintained in DMEM/F-12 media with L-glutamine (Mediatech), supplemented with 10% (v/v) fetal bovine serum (FBS, Hyclone), 50 units/ml penicillin, and 50 μg/ml streptomycin (BioWhittaker). To monitor HIF-1 activity, a T47D cell-based luciferase assay employing the pHRE3-TK-Luc reporter was performed as described (29). A similar cell-based luciferase reporter assay was conducted with a control construct (pGL3-Control, Promega). Compounds were prepared as stock solutions in DMSO and stored in aliquots at −80 °C. The final concentration of DMSO is less than 0.5% (v/v) in all assays.

RNA Extraction and Quantitative Real Time RT-PCR—The plating of T47D cells, compound treatment, extraction of total RNA samples, synthesis of the first strand cDNAs, gene-specific primer sequences, quantitative real time PCRs, and data analysis were described previously (30).

ELISA for Human VEGF Protein—The plating of T47D cells, compound treatment, and ELISA for secreted and cellular VEGF proteins were the same as those described previously (29). The protein concentration of the cellular lysate was determined using a micro BCA assay (Pierce), and the amount of VEGF protein was normalized to that of proteins in the cellular lysate.

HUVEC Cell Tube Formation Assay—HUVEC cells (Lonza) were maintained in endothelial cell basal medium (EBM-2, Lonza) supplemented with 5% (v/v) FBS (Hyclone) and endothelial cell growth supplement (SingleQuots, Lonza). Only cells within six passages were used. To collect conditioned media (CM) samples, T47D cells were plated at the density of 10^6 cells/well (6-well plate, Cellstar) in a volume of 2 ml of DMEM/F-12 media supplemented with 10% FBS and antibiotics, incubated overnight, and exposed to compounds under normoxic (95% air) and hypoxic conditions (1% O_2) for 24 h; the CM were centrifuged at 3,000 × *g* for 5 min at 4 °C, and the supernatant samples were stored at −80 °C. For the *in vitro* tube formation assay, 60,000 HUVEC cells/well were added to a Matrigel (BD Biosciences)-coated 24-well plate (Cellbind, Corning Inc.). The cells were added in a volume of 1 ml of EBM-2 media as a negative control and EBM-2 media supplemented with 20 ng of recombinant human VEGF protein (R & D Systems) as a positive control. For the rest, HUVEC cells were added in a mixture of EBM-2 (800 μl) and T47D cell-conditioned media (200 μl, thawed on ice). The incubation was continued for another 18 h at 37 °C. The HUVEC cells/tubes were washed with 1× phosphate-buffered saline, fixed with cold methanol for 10 s, and stained with Diff-Quik II (Dade Behring). Three random fields of each sample were photographed under an Axiovert 40 CFL microscope (Zeiss). Both the tube length and the number of branching points were quantified using Adobe Photoshop. The tube length measurements were presented as percentage of the normoxic control.

MDA-MB-231 Cell-based Wound Healing and Chemotaxis Assays—MDA-MB-231 cells were plated at the density of 10^6 cells/well into 12-well plates (Corning Inc.). After 24 h, three parallel wounds were created inside each well by scratching the layer of confluent MDA-MB-231 cells with a 200-μl pipette tip at a 90° angle. The cells were washed twice with a serum-free medium, and a fresh DMEM/F-12 medium supplemented with 5% (v/v) FBS (Hyclone), penicillin/streptomycin, and each specific test compound was added. Following a short incubation (30 min at 37 °C), the exposure was extended for another 22–24 h under specified oxygen conditions (normoxia, 95% air, 5% CO_2; hypoxia, 1% O_2, 94% N_2, 5% CO_2). When the wound healed in the control wells, the cells were fixed with methanol and stained with 0.1% crystal violet. The wounds were photographed under a Zeiss Axiovert 40 microscope.

The migration of MDA-MB-231 cells toward fetal bovine serum was measured using a QCM™ 24-well cell migration assay kit (Chemicon International). Serum-starved MDA-MB-231 cells were seeded at the density of 10^5 cells per insert (8.0 μm pore size) in a volume of 300 μl serum-free DMEM/F12 media with antibiotics. The inserts were placed into a 24-well plate with 500 μl of 10% FBS media with antibiotics per well. Compounds were added to both the insert and the lower chamber, and the cells were exposed to specified oxygen conditions for 24 h. Cell detachment, lysis, and labeling with the CyQuant GR fluorescent dye were performed following the manufacturer's instruction. Fluorescence was measured on a BioTech Synergy Plate Reader with excitation at 480 nm and emission at 520 nm. The number of cells was calculated from a standard curve.

Nuclear Extract Preparation and Western Blot Analysis—Plating of T47D cells, compound treatment, and exposure to hypoxic conditions were described (29). Nuclear extract samples were prepared using NE-PER nuclear and cytoplasmic extraction kit (Pierce), and the protein concentration was determined using a Micro BCA assay kit (Pierce). Each sample (60 μg) was separated by electrophoresis on an 8% SDS-polyacrylamide gel, and the proteins were transferred onto a nitrocellulose membrane (Bio-Rad) using a Bio-Rad semi-dry blotter. The membrane was blocked in 5% nonfat milk (Bio-Rad) in TTBS (20 mM Tris, pH 6.8, 150 mM NaCl, 0.05% Tween 20) at 4 °C overnight and incubated with specified primary antibodies in TTBS with 1% bovine serum albumin at room temperature for 1 h. Both monoclonal anti-HIF-1α antibody (1:500) and monoclonal anti-HIF-1β antibody (1:1000) were from BD Biosciences. The secondary antibody (ECL™-horseradish peroxidase-linked sheep anti-mouse IgG, Amersham Biosciences) was used at 1:30,000. The blot was developed with the Super-Signal West Femto Maximum Sensitivity Substrate (Pierce).

In Vitro Translation—Coupled *in vitro* transcription/translation of the luciferase T7 control DNA construct (Promega) was performed in a final volume of 12.5 μl using the TnT® T7 coupled reticulocyte lysate system (Promega) following the manufacturer's instructions. Compounds were added before addition of the lysate. One-fifth of the reaction mix was used for luciferase activity determination (Luciferase assay system, Promega).

Mitochondria Respiration Assay—To determine the effect of each isolated compound on cell respiration, 5×10^6 T47D cells (equilibrated to 30 °C) were added to the chamber of an Oxytherm Clark-type electrode system (Hansatech) containing 1 ml of DMEM/F-12 medium (JRH) free of serum and antibiotics. Glucose (17.5 mM) in the DMEM/F-12 media served as the metabolic substrate. Once base-line respiration had been established (for a 15-min interval), compounds dissolved in DMSO were injected into the chamber at 3-min intervals using a 100-μl syringe (Hamilton). For mechanistic studies, the plasma membrane was selectively permeabilized with digitonin (30 μM) so that the substrates available to the mitochondria could be manipulated. This required the use of a mitochondrial buffer containing 20 mM HEPES, pH 7.3, 120 mM KCl, 2 mM KH_2PO_4, 2 mM $MgCl_2$, 1 mM EGTA, and 0.3% bovine serum albumin (fat-free) in place of the DMEM/F-12 medium. The buffer was supplemented with the following substrates that provide electrons to different sites within the mitochondrial respiratory chain: 5 mM sodium pyruvate and 5 mM sodium malate (complex I), 5 mM sodium succinate dibasic hexahydrate (complex II), and 5 mM L-ascorbic acid plus 0.2 mM *N,N,N′,N′*-tetramethyl-*p*-phenylenediamine (complex IV). Known complex I and III inhibitors, rotenone and antimycin A, respectively, were added from EtOH stock solutions to a final concentrations of 1 μM where indicated. All the chemicals were from Sigma, and the final concentration of solvent was less than 0.1% (v/v).

Cell Viability Assays—The plating of cells, compound treatment, and exposure to hypoxic conditions were similar to those described in the earlier sections. For the 6-day exposure study, the conditioned media were replaced by fresh culture medium that contained test compound after 3 days. Following a 2- or 6-day incubation period, cell viability was determined by one of the following methods as appropriate. For the MTT assay, the conditioned media were replaced with a fresh DMEM/F-12 medium that contains 10% FBS, penicillin/streptomycin, and MTT (0.5 mg/ml). After 4 h of incubation at 37 °C, the media were removed, and the cells were lysed with isopropyl alcohol that contains 0.04 N HCl. Absorbance at 570 nm was measured on a BioTek Synergy plate reader with background absorbance at 690 nm. For direct cell number counting, cells plated in 12-well plates were trypsinized, the plates kept on ice, and the cell numbers counted using a hemocytometer.

Statistical Analysis—Data were compared using one-way ANOVA and Bonfferoni post hoc analyses (GraphPad Prism 4). Differences were considered significant when $p < 0.05$.

RESULTS

*Alpinumisoflavone (**1**) and 4′-O-Methylalpinumisoflavone (**2**) Inhibit HIF-1 Activation in T47D Cells*—Over 15,000 natural product-rich extracts from plants, marine invertebrates, algae, and microorganisms were evaluated in a T47D human breast tumor cell-based reporter assay for HIF-1 inhibitory activity (29). The lipid extract from the plant *L. glabrescens* Benth (Facaceae) inhibited hypoxia (1% O_2)-induced HIF-1 activation by 90% at the concentration of 0.5 μg/ml. Bioassay-guided chromatographic separation of the active extract yielded two new HIF-1 inhibitors. The HIF-1 inhibitors isolated were determined to be alpinumisoflavone (**1**) and 4′-*O*-methylalpinumisoflavone (**2**) (Fig. 1*A*) by direct comparison of the spectroscopic data with previously published values (31). A concentration-response study was performed in T47D cells to determine the effects of compounds **1** and **2** on HIF-1 activation using cell-based reporter assays (Fig. 1*B*). Rotenone (**3**), a structurally similar compound from the same plant, was used as a control that is believed to inhibit hypoxia-induced HIF-1 activation by blocking the mitochondrial electron transport chain (ETC) (32). Unlike compound **3**, compounds **1** and **2** inhibited both hypoxia-induced (1% O_2) and iron chelator-induced HIF-1 activation with comparable low micromolar IC_{50} values (Fig. 1, *B* and *D*). Expression of luciferase from a control construct (pGL3-Control) was only modestly suppressed by compounds **1** and **2** (IC_{50} >10 μM, data not shown). Compound **3** only inhibited hypoxia (1% O_2)-induced HIF-1 activation (IC_{50} 0.001 μM) and had little effect on iron chelator (10 μM 1,10-phenanthroline)-induced HIF-1 activation (IC_{50} >0.1 μM) (Fig.

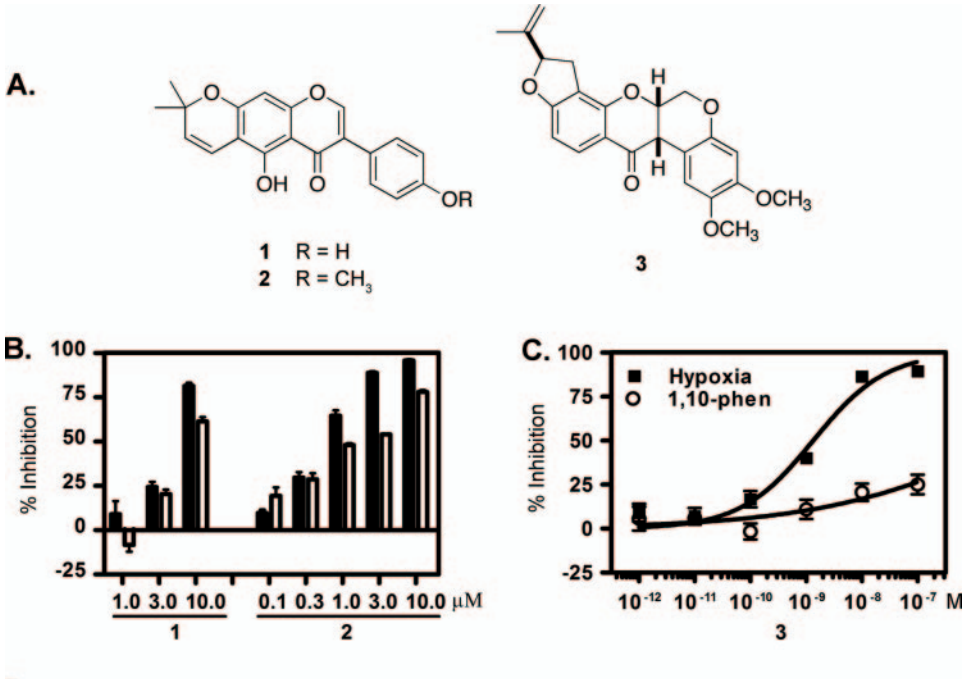

D. IC_{50} (μM):

Reporter Construct / Inducing Conditions	alpinumisoflavone (1)	methylalpinumisoflavone (2)	rotenone (3)
pHRE-luc/1% O_2	5.0	0.6	0.001
pHRE-luc/1,10-phen	7.5	1.5	> 0.1

FIGURE 1. **Structures and inhibition of HIF-1 activation by compounds 1–3.** *A*, chemical structures of two newly identified HIF-1 inhibitors isolated from *L. glabrescens*: alpinumisoflavone (**1**) and 4′-*O*-methylalpinumisoflavone (**2**), and rotenone (**3**). *B* and *C*, concentration-response results in T47D cell-based reporter assays for HIF-1 activity (the inducing conditions are hypoxia (1% O_2, *black bar*) and 1,10-phenanthroline (10 μM, *open bar*)). Averages from one representative experiment performed in triplicate are shown, and the *error bars* indicate standard deviation. *D*, IC_{50} values (μM) of **1–3** derived from *B* and *C*.

1, *C* and *D*). The observation that compound **2** is eight times more potent than **1** at inhibiting hypoxia-induced HIF-1 activation suggests that the 4′-*O*-methyl substituent contributes to the enhanced activity. A similar difference in relative potency was observed between **1** and **2** in their abilities to inhibit 1,10-phenanthroline-induced HIF-1 activation (**2** was five times more potent than **1**). Because **1** and **2** differ by only one methyl group and **2** was significantly more potent, the subsequent studies were mainly performed with **2**.

The effects of **2** and **3** on the expression of HIF-1 target genes *CDKN1A* (Fig. 2*A*), *GLUT-1* (Fig. 2*B*), and *VEGF* (Fig. 2*C*) were examined in T47D cells by real time RT-PCR. At the minimum inhibitory concentration (MIC) value determined in the T47D cell-based reporter assay, compound **2** (10 μM) blocked the hypoxic (1% O_2) induction of all three HIF-1 target genes at the mRNA level, but exerted only modest effects (15–24% inhibition) on target gene induction by 1,10-phenanthroline (10 μM). One explanation for the reduced ability of compound **2** to inhibit 1,10-phenanthroline-induced HIF-1 target gene expression is that higher concentrations are required to inhibit HIF-1 target gene expression than those to inhibit HIF-1 activation in the reporter-based assay. Compound **3** inhibited hypoxic induction of all three genes (complete inhibition for *CDKN1A*, 63% for *GLUT-1*, and 81% for *VEGF*) at concentrations as low as 10 nM (MIC value to inhibit HIF-1 activation by hypoxia in the reporter assay). In sharp contrast to its effect on hypoxia-induced HIF-1 activation, compound **3** only modestly inhibited the induction of all three genes by 1,10-phenanthroline (30–40% inhibition) even at a concentration of 100 nM. The relatively hypoxia-selective inhibitory effects of **3** on HIF-1 target gene induction at the mRNA level mirror the results observed in the T47D cell-based reporter assay.

4′-O-Methylalpinumisoflavone (2) and Rotenone (3) Inhibit Hypoxic Induction of VEGF Protein and Tumor Angiogenesis in Vitro—One of the survival mechanisms employed by hypoxic tumor cells is to increase the production of angiogenic factors such as VEGF, which serves as a trigger to initiate the process of tumor angiogenesis. To test whether **2** and **3** can inhibit hypoxic induction of VEGF protein, the levels of both cellular (Fig. 3*A*) and secreted (Fig. 3*B*) VEGF proteins were measured. In T47D cells, hypoxic exposure significantly increases the levels of both cellular and secreted VEGF proteins. Compound **2** (10 μM) completely blocked the hypoxic induction of both cellular and secreted VEGF proteins ($p > 0.05$, when the hypoxia plus compound **2** treatment was compared with the normoxic control using ANOVA and Bonferroni's post test, GraphPad Prism). Compound **3** inhibited hypoxic induction of cellular and secreted VEGF proteins at the concentration of 100 nM. Neither **2** nor **3** inhibited the induction of VEGF proteins by 1,10-phenanthroline (10 μM, chemical hypoxia). The less active compound **1** did not inhibit the induction of VEGF proteins in T47D cells when tested at 10 μM (data not shown). These results parallel the results observed in the T47D cell-based reporter assay.

To investigate if the inhibition of VEGF protein production correlates with the inhibition of tumor angiogenesis, a HUVEC-based *in vitro* angiogenesis assay was utilized for the follow-up study. In the absence of stimuli, HUVEC cells are scattered throughout the plate (Fig. 3*C*, *Basal Media*). Addition of the angiogenic factor VEGF stimulated the HUVEC cells to form a network of tube-like structures (Fig. 3*C*, *VEGF*). Similar angiogenesis inducing activity was observed in the presence of conditioned media collected from T47D cells cultured under normoxic conditions (Fig. 3*C*, *Control, Normoxia*). Conditioned media collected from hypoxic T47D cells exhibited a significantly enhanced angiogenesis stimulating activity (Fig. 3*C*, *Control, Hypoxia*). Compound **2** inhibited the ability of

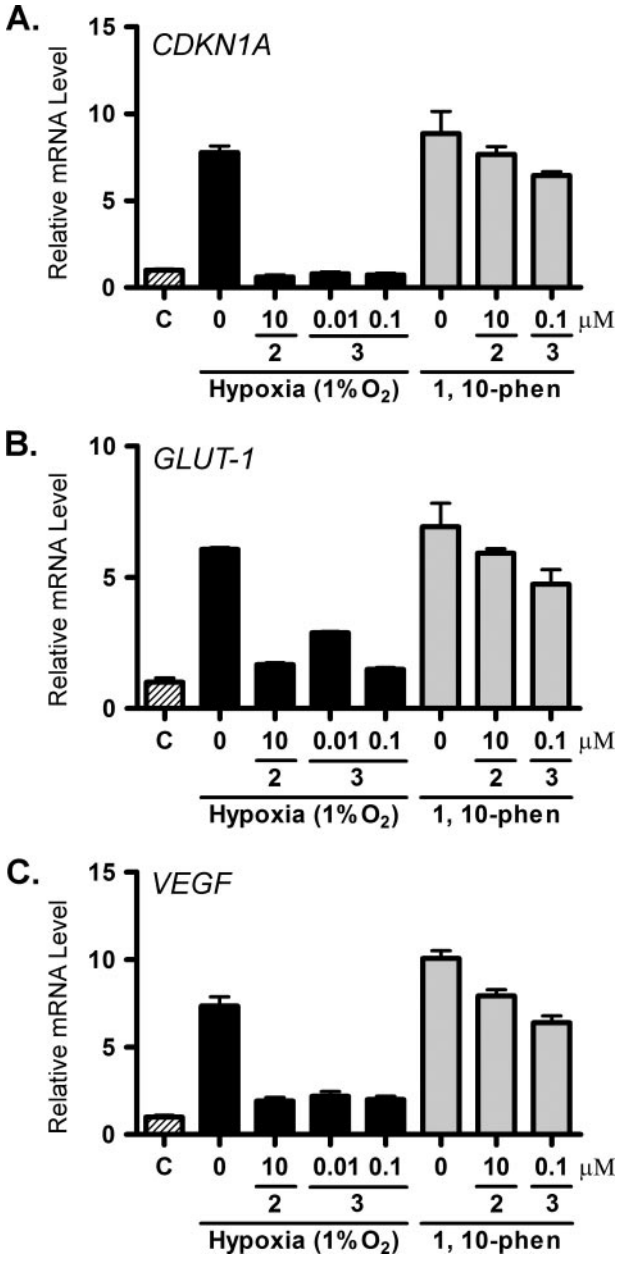

FIGURE 2. **Compounds 2 and 3 inhibit the induction of HIF-1 target genes.** T47D cells were exposed to hypoxia or 1,10-phenanthroline (*1,10-phen*) in the presence of compound **2** or **3** for 16 h and the total RNA samples were isolated. The levels of *CDKN1A* (*A*), *GLUT-1* (*B*), and *VEGF* (*C*) mRNA in each sample were quantified by real time RT-PCR. The data (mean ± S.D., $n = 3$) are normalized to an internal control (18 S rRNA) and presented as relative mRNA level of the normoxic control.

hypoxic T47D cells to stimulate tumor angiogenesis (Fig. 3*C*, **2** (10 μM), *Hypoxia*). Compound **3** suppressed hypoxic T47D cell-stimulated tumor angiogenesis at concentrations as low as 10 nM (Fig. 3*C*, **3** (0.01 μM) and **3** (0.1 μM), *Hypoxia*). These observations correlate with the inhibitory effects exerted by **2** and **3** on hypoxic induction of secreted VEGF proteins in T47D cells (Fig. 3*B*). Two criteria that are used to quantify the extent of angiogenesis in the HUVEC tube formation assay are the length of the tubes and the number of branching points. Neither **2** nor **3** decreased tumor angiogenesis under normoxic conditions ($p > 0.05$, when both the tube length and the number of branching points observed in the compound treated samples were compared with those of the control using ANOVA and Bonferroni's post test, GraphPad Prism). Both **2** and **3** suppressed hypoxic T47D cell-induced angiogenesis (Fig. 3*D*, *tube length*; Fig. 3*E*, *number of branching points*). Compound **2** inhibited tumor angiogenesis associated with hypoxic cells to a level less than that observed with normoxic cells.

*Alpinumisoflavone (**1**) and 4′-O-Methylalpinumisoflavone (**2**) Inhibit MDA-MB-231 Cell Migration and Chemotaxis*—Hypoxia represents a physiological stimulus for tumor cell invasion and metastasis, and HIF-1 has been shown to regulate multiple steps throughout the complex metastatic process (33). Because compounds **1**–**3** inhibited hypoxia-induced HIF-1 activation, their effects on tumor cell migration were first examined in a wound-healing assay. The metastatic human breast tumor MDA-MB-231 cells were used as an *in vitro* model for this study. A wound was created in a confluent layer of MDA-MB-231 cells using a pipette tip (Fig. 4*A*, T_0). Over a 22-h period, MDA-MB-231 cells migrated into the scratched area and resulted in "healing" of the wound (Fig. 4*A*, *Control*). Compounds **1** (30 μM) and **2** (10 μM) suppressed MDA-MB-231 cell migration under both normoxic (95% air) and hypoxic (1% O_2) conditions (Fig. 4*A*, **1** (30 μM) and **2** (10 μM)). Although compounds **1** and **2** differ by only one methyl substituent, compound **2** more potently inhibited both HIF-1 activation and tumor cell migration. Compound **3** did not inhibit MDA-MB-231 cell migration even at a concentration of 100 nM (data not shown), although it potently inhibited hypoxic activation of HIF-1 in T47D cells (IC_{50} 1 nM, MIC 10 nM).

Hypoxic tumor cells are often deprived of growth factors, and this lack of growth factors promotes them to migrate toward growth factor-rich environments (chemotaxis, a major event in the process of metastasis). A modified chemotaxis assay was performed to examine the effects of compounds **1**–**3** on the migration of serum-starved MDA-MB-231 cells toward growth factors present in the FBS. As shown in Fig. 4*B*, all three compounds inhibited the chemotaxis of serum-starved MDA-MB-231 cells under both normoxic and hypoxic conditions.

*4′-O-Methylalpinumisoflavone (**2**) and Rotenone (**3**) Inhibit Hypoxic Induction of HIF-1α Protein via Different Mechanisms*—One key event leading to the activation of HIF-1 is the induction of HIF-1α protein in the nucleus. A number of small molecule natural products inhibit HIF-1 activation by blocking the induction of HIF-1α protein (34). Compounds **1**–**3** were examined for their effects on hypoxic induction of nuclear HIF-1α protein in T47D cells. At concentrations that inhibit both HIF-1 activation and the induction of HIF-1 target genes, compounds **2** (10 μM) and **3** (0.01 and 0.1 μM) inhibited hypoxic induction of nuclear HIF-1α protein without significantly affecting the constitutively expressed nuclear HIF-1β protein (Fig. 5*A*). Less than a 20% difference was observed between the compound-treated samples and the control on the HIF-1β Western blot (the image in Fig. 5*A* was quantified using Image J (National Institutes of Health) and the density of the band compared, data not shown). Neither **2** nor **3** decreased the levels of *HIF-1A* mRNA under hypoxic conditions (16 h, non-cytotoxic concentrations, Fig. 5*B*). Thus, it is logical to conclude that **2**

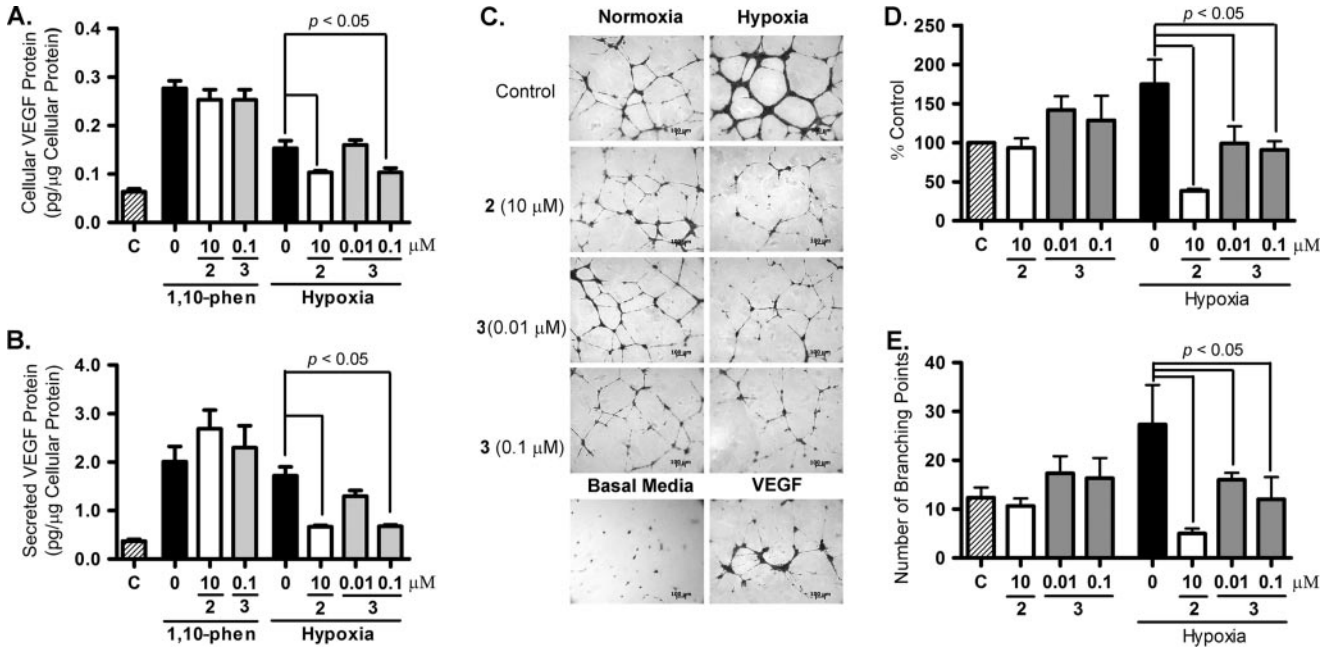

FIGURE 3. **Compounds 2 and 3 inhibit the induction of VEGF proteins and tumor angiogenesis *in vitro*.** Levels of cellular VEGF protein in the cell lysate (*A*) and secreted VEGF protein in the conditioned media (*B*) from T47D cells exposed to hypoxia or 1,10-phenanthroline (*1,10-phen*) in the presence of compounds **2** or **3** (16 h) were determined by ELISA and normalized to the amounts of cellular proteins. Data shown are averages from one representative experiment performed in triplicate, and the *bars* indicate standard deviation. The *p* values are provided when there is a statistically significant difference between the induced and the compound-treated samples. The effects of T47D cell-conditioned media on angiogenesis were evaluated in a HUVEC tube formation assay (*C*). Representative pictures are shown, and each panel includes a 100-μm *scale bar*. The negative (*Basal Media*) and positive (*VEGF*) controls are included at the *bottom*. The extent of tube formation in three randomly selected fields was quantified for each condition in *C*. The data shown are averages, and the *bars* represent standard deviation (tube length (*D*) and number of branching points (*E*)). The *p* values are provided where there is a statistically significant difference ($p < 0.05$) between the hypoxic control (*C*) and the compound-treated samples.

and **3** decrease HIF-1α protein levels through mechanisms related to translation and/or post-translational modifications but do not directly affect transcription and/or mRNA stability. Compounds **1–3** were examined for their effects on overall protein synthesis in a coupled *in vitro* transcription/translation system (TnT® T7 system, Promega) (Fig. 5*C*). In this system, the relative luciferase activity correlates with the level of luciferase expression from the luciferase T7 control DNA construct (Promega). Compound **2** exhibited concentration-dependent inhibition of luciferase expression (19% at 1 μM and 51% at 10 μM), whereas neither **1** (10 μM) nor **3** (0.01 and 0.1 μM) inhibited protein synthesis in this *in vitro* system. Thus, inhibition of protein synthesis in general constitutes one mechanism for compound **2** to inhibit nuclear HIF-1α protein accumulation in T47D cells. Mitochondria inhibitors constitute one important group of small molecule HIF-1 inhibitors (34). The *Lonchocarpus* metabolite rotenone (**3**) is known to inhibit the mitochondrial respiratory chain by inhibiting NADH-ubiquinone oxidoreductase (complex I). Although the structure of **2** is only remotely similar to that of **3**, the effect of **2** on cellular oxygen consumption was examined in T47D cells (Fig. 5*D*). Compound **2** suppressed oxygen consumption at the concentrations that inhibited HIF-1 activation (1–10 μM). In contrast, the structurally related compound **1** (10 μM) that did not inhibit HIF-1 activation also failed to suppress oxygen consumption (data not shown). The concentrations of compound **3** required to inhibit oxygen consumption correlate with the concentrations observed to inhibit HIF-1 activation in T47D cells (1–100 nM).

Mechanistic studies were performed to discern where within the ETC compound **2** acts to inhibit electron transport (Fig. 5, *E* and *F*). A mixture of malate and pyruvate was added to permeabilized T47D cells to initiate mitochondrial respiration at complex I (NADH-ubiquinone oxidoreductase). This respiration was inhibited by the complex I inhibitor rotenone (Fig. 5*E*). Succinate, a substrate for complex II, overcomes the inhibition exerted by complex I inhibitors (*e.g.* rotenone). The observation that compound **2** did not affect mitochondrial respiration in the presence of succinate indicated that compound **2** does not inhibit complex II, III, or IV. To ensure that the ETC remained functional, the complex III inhibitor antimycin A was added to inhibit respiration, and complex IV substrates *N*,*N*,*N*′,*N*′-tetramethyl-*p*-phenylenediamine/ascorbate were added to re-initiate respiration (Fig. 5*E*). As in the case of the mitochondrial complex I inhibitor rotenone, addition of the complex II substrate succinate reestablishes mitochondrial respiration and electron transport following inhibition with compound **2** (Fig. 5*F*). Overall, the data presented in Fig. 5, *E* and *F*, indicate that compound **2** selectively inhibits mitochondrial ETC at complex I. Thus, compound **2** inhibits HIF-1 activation through at least two mechanisms, reduction of mitochondria complex I-mediated respiration and inhibition of protein synthesis, whereas rotenone (**3**) primarily affects mitochondrial respiration.

*Effects of Alpinumisoflavone (**1**), 4′-O-Methylalpinumisoflavone (**2**), and Rotenone (**3**) on Tumor Cell Proliferation/Viability under Normoxic and Hypoxic Conditions*—Concentration-response studies were performed to evaluate the effects of

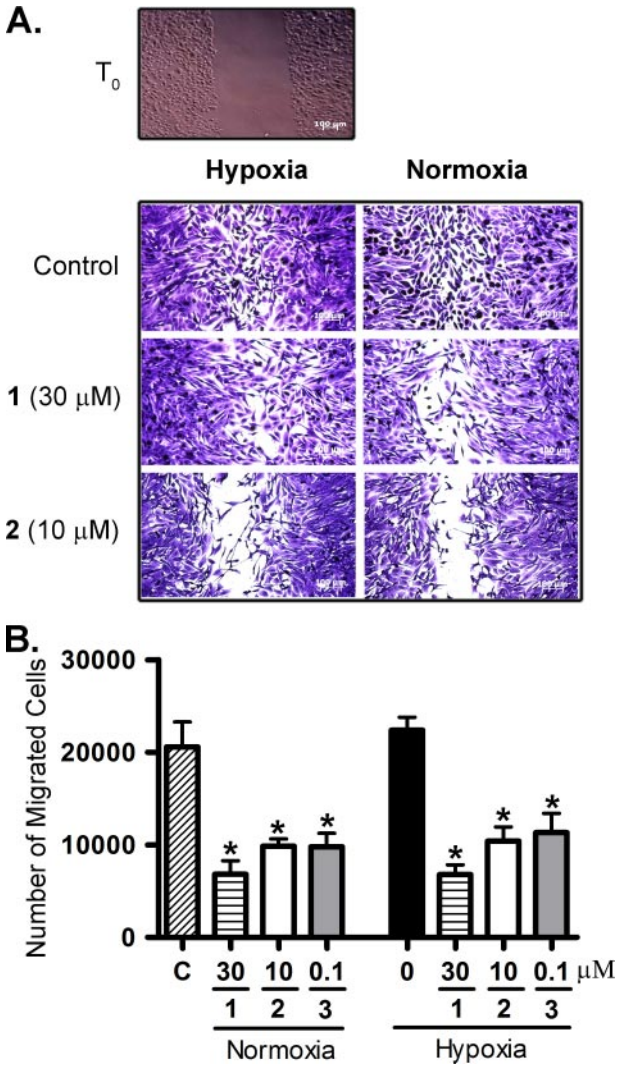

FIGURE 4. **Effects of compounds 1-3 on MDA-MB-231 cell migration and chemotaxis.** *A,* healing of a wound on a confluent layer of MDA-MB-231 cells was examined in the presence and absence of compounds under normoxic (95% air) and hypoxic (1% O_2) conditions. A photograph of the wound at T_0 is shown at the *top* of *A*. The cells were fixed and stained with crystal violet. Each panel includes a 100-μm *scale bar*. *B,* effects of compounds **1** (30 μM), **2** (10 μM), and **3** (100 nM) on the chemotaxis of serum-starved MDA-MB-231 cells toward FBS were evaluated under both normoxic and hypoxic conditions. Data shown are averages of the number of migrated cells ($n = 3$), and the *bars* represent standard deviation. An *asterisk* indicates $p < 0.05$ when compared with the control (*C*).

compounds **1**–**3** on tumor cell proliferation/viability under normoxic and hypoxic conditions. The compounds were tested at a range of concentrations as follows: **1** and **2** (10^{-7} to 10^{-5} M in half-log increments), and **3** (10^{-14} to 10^{-7} M in single-log increments). In human breast tumor MDA-MB-231, human prostate tumor PC-3, and DU-145 cells, none of the compounds affected cell proliferation/viability by greater than 30% relative to the control following 48 h of incubation under either normoxic or hypoxic conditions (supplemental Fig. S1). In T47D cells, neither compound **1** nor **2** inhibited cell viability at the concentration of 10 μM, regardless of the oxygen conditions (Fig. 6*A*). Compound **3** did not inhibit T47D cell proliferation/viability at the MIC value (10 nM) for HIF-1 inhibition, but it did decrease cell viability/proliferation by ~60% at 100 nM after 48 h (Fig. 6*A*). No significant cytotoxicity (<20%) was observed following a 16-h exposure that was used in both reporter assay and downstream target gene expression. An extended cell proliferation/viability study (6 day) suggests that T47D cells are more sensitive to the growth inhibitory effects of these compounds, in comparison with MDA-MB-231 cells (Fig. 6*B*).

DISCUSSION

Natural products continue to be a major source of small molecule-based drug leads and have served as valuable molecular probes in biomedical research (35). To discover natural product-derived inhibitors of HIF-1 activation, a combined approach was utilized that incorporated the unrivaled biochemical diversity afforded by natural products with tumor cell-based screening assays (29). Plant and marine organism extracts were evaluated in the human breast tumor T47D cell-based reporter assay for HIF-1 inhibitory activity. Active extracts identified in the primary assay were subsequently subjected to a panel of confirmatory bioassays, and pure compounds were isolated from active extracts following bioassay-guided separation. The chemical structures of active compounds elucidated using a combination of spectroscopic and spectrometric methods and the pharmacological activities of the purified natural products were investigated using established tumor cell lines as *in vitro* models.

This report details the discovery and characterization of two small molecule HIF-1 inhibitors from the plant *L. glabrescens* using such a combined approach. In the T47D cell-based primary assay, the lipid extract of *L. glabrescens* inhibited hypoxia (1% O_2)-induced HIF-1 activation without exhibiting any pronounced cytotoxicity. The genus *Lonchocarpus* is known to contain rotenoids including rotenone (**3**) (36). Previous studies on the role of mitochondria in hypoxia-induced HIF-1 activation have shown that the complex I inhibitor rotenone can inhibit HIF-1 activation (32, 37). To determine whether other natural products also contribute to the potent HIF-1 inhibitory activity of *L. glabrescens* extract, initial bioassay-guided isolation efforts were specifically directed at the active fractions that were devoid of rotenone. Chromatographic separation of the active fractions by reverse phase high performance liquid chromatography yielded two isoflavanoids alpinumisoflavone (**1**) and 4′-*O*-methylalpinumisoflavone (**2**). Relatively little is known regarding the potential pharmacological activities associated with either of these isoflavone metabolites. The few published observations indicate the following: (*a*) compounds **1** and **2** weakly inhibit mouse brain monoamine oxidase *in vitro* (IC_{50} values 25.8 and 23.9 μM, respectively) (38); (*b*) compound **1** weakly inhibits recombinant human protein-tyrosine phosphatase 1B in an enzyme-based assay with an IC_{50} value of 42 μM (39); and (*c*) compound **2** exhibits brine shrimp toxicity at high concentrations (LD_{50} 100 μM) (40). From these studies with relatively high concentrations of each compound, it is difficult to discern the overall impact of these compounds in relevant biological systems. The studies described herein represent the first account of the anti-tumor activities of these isoflavanoid natural products in molecular-targeted tumor cell-based systems. Compound **2**, the 4′-*O*-methylated form of **1**, was significantly more potent than **1**. One possible explanation

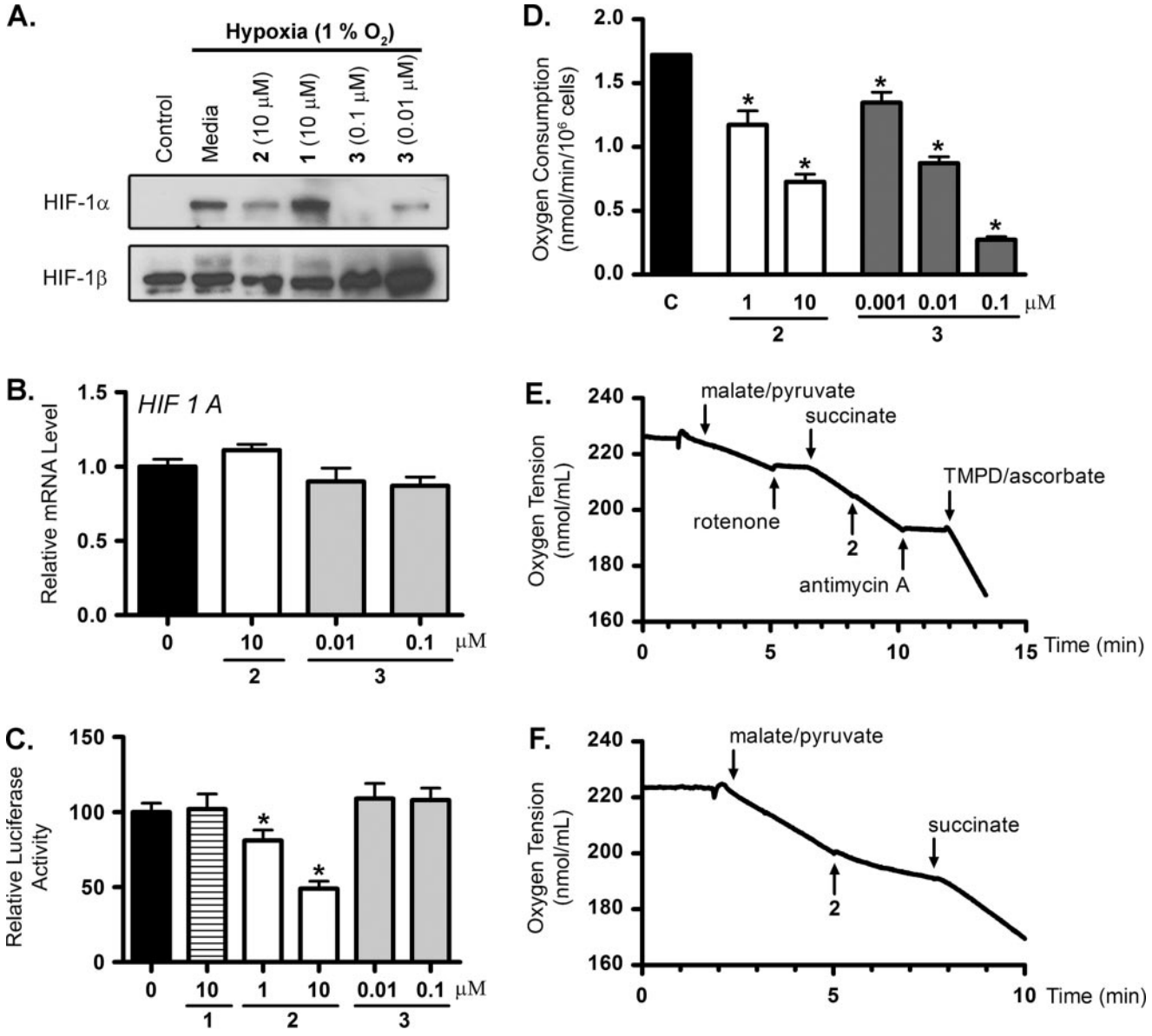

FIGURE 5. **Mechanisms of action for compounds 2 and 3 to inhibit HIF-1 activation.** *A,* Western blot analysis of HIF-1α and HIF-1β proteins in nuclear extract samples prepared from T47D cells. *B,* real time RT-PCR analysis for the levels of *HIF1A* mRNA in the presence and absence of compounds under hypoxic conditions (1% O_2, 16 h). *C,* effects of compounds **1–3** on protein synthesis *in vitro* in a TNT® coupled transcription/translation system. Luciferase activity correlates to the level of luciferase expression from a control construct in the presence and absence of compounds. Data shown are averages from one experiment performed in triplicate and the *bars* represent standard deviation. An *asterisk* indicates $p < 0.05$ when compared with the control. *D,* compounds **2** and **3** inhibit oxygen consumption in T47D cells. Data shown are averages from three independent experiments, and the *bars* indicate standard deviation. An *asterisk* indicates $p < 0.05$ when compared with the control (*C*). *E,* compound **2** (10 μM) does not affect complex II, III, or IV. Substrates and inhibitors were added to T47D cells (5×10^6, 30 °C) at the time point specified in a sequential manner. *F,* compound **2** (10 μM) inhibits mitochondria respiration by targeting complex I.

for this difference in potency is that 4′-*O*-methylation increases the lipophilic nature of this compound and may enhance its cellular penetration.

There are opposing theories on the role of mitochondria in mediating hypoxic signaling, each supported by a body of experimental evidence. One theory suggests that reactive oxygen species (ROS) generated by mitochondria mediate hypoxia-induced HIF-1 activation (32, 41). The other theory asserts that the mitochondrial ETC is not essential for the hypoxia-induced HIF-1 activation (37). Recent studies employing a genetic-based approach support the hypothesis that mitochondrial ROS mediate hypoxic HIF-1 activation (42, 43). Distinctly different cell lines and oxygen concentrations were used in the early studies that led to the opposing theories. Therefore, it is possible that the controversial role of the mitochondria in regulating hypoxia sensing and signaling may have arisen from cell line-specific and/or hypoxic condition-dependent variations in previously reported experiments. Other investigators have demonstrated that mitochondria are required for hypoxic HIF-1 activation but are not required to activate HIF-1 under anoxic conditions (44, 45). Inhibitors of mitochondrial respiration such as rotenone have been used as molecular probes to investigate the role of mitochondria in hypoxic signaling. However, most of these studies have not established cell line-specific

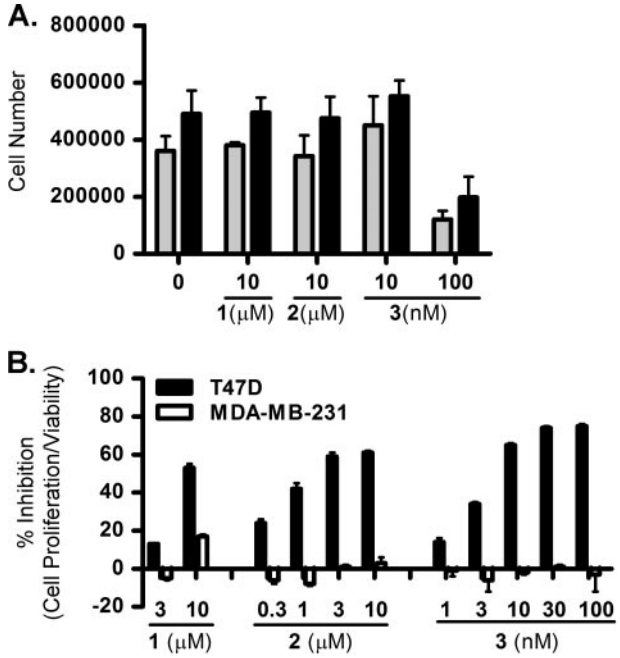

FIGURE 6. **Effects of compounds 1-3 on cell proliferation/viability.** *A,* effects of compounds **1–3** on T47D cell proliferation/viability under normoxic and hypoxic conditions. Cells were exposed to normoxic (95% air, *gray bar*) and hypoxic (1% O_2, *black bar*) conditions for 48 h in the presence and absence of compounds. The number of viable cells was counted using a hemocytometer. The *error bars* indicate standard deviation in a representative experiment performed in triplicate. *B,* effects of compounds **1–3** on T47D and MDA-MB-231 cell proliferation/viability after a 6-day exposure. Cell viability was determined with a modified MTT assay and presented as % inhibition using the following formula: % inhibition $= 1 - A_{570(\text{Treated})}/A_{570\ (\text{Control})}$. Data shown are averages from one representative experiment performed in triplicate, and the *bars* represent standard deviation.

concentration-response curves, but have typically used rotenone at a single test concentration (*e.g.* micromolar) (32). Vaux *et al.* (37) performed concentration-response studies and found that rotenone reduced hypoxic (0.1% O_2) induction of HIF-1α protein at a concentration that was 100 times the concentration that inhibited oxygen consumption in Chinese hamster ovary CHO-K1 cells. Our studies indicate that rotenone inhibits both mitochondrial respiration and hypoxic (1% O_2) induction of HIF-1α protein at similar concentrations in T47D cells (Fig. 5, *A* and *D*). The concentration of rotenone required to suppress HIF-1α protein accumulation was 0.01 μM in T47D cells, in comparison with 10 μM in CHO-K1 cells (37). Genetic differences between the two cell lines (T47D in our study and CHO-K1 in theirs) may contribute to the reduced potency of rotenone. Another important factor may lie in the specific hypoxic conditions used in each study: the 0.1% oxygen concentration used in their study is significantly closer to anoxia relative to our studies that were conducted under 1% oxygen conditions. In fact, these results coincide with the studies that indicate mitochondria affect hypoxia-induced HIF-1 activation but not anoxia-induced HIF-1 activation (44, 45). Recent evidence indicates that, under hypoxic conditions, ROS released by complex III of the mitochondrial ETC act as "hypoxic signaling molecules" that activate HIF-1 by deactivating the prolyl hydroxylases that initiate the proteasome-mediated degradation of HIF-1α protein (41–43, 46). According to this model, mitochondrial inhibitors (*e.g.* rotenone) are believed to suppress hypoxia-induced HIF-1 activation by blocking the mitochondrial ETC at any number of specific sites upstream of complex IV (*e.g.* rotenone inhibits complex I), thus preventing the release of ROS from mitochondrial ETC complex III into the mitochondrial intermembrane space. This model is further supported by the identification and characterization of mitochondrial inhibitors from a chemical genomics screen for small molecule HIF-1 inhibitors (47).

One important observation is that compound **2** inhibits HIF-1 activation via dual mechanisms. Most of the dual inhibitors that are under preclinical/clinical evaluation affect a single class of molecular/biochemical targets (*e.g.* kinases) (48). Compound **2** is unique in the aspect that this natural product inhibits both mitochondrial respiration and protein synthesis. In contrast, other structurally related HIF-1 inhibitors such as the plant isoflavone genistein and the synthetic flavone PD98059 are protein kinase inhibitors (49, 50). When evaluated in a panel of 80 different kinase assays *in vitro* (NovaScreen Biosciences, Hanover, MD), compound **2** did not exert significant inhibition of any specific kinase at the concentration of 3 μM that inhibited hypoxic activation of HIF-1 by 90%.[4] This is the first example of a small molecule HIF-1 inhibitor that targets multiple cellular processes at the concentrations that inhibit HIF-1 activation. As a consequence, compound **2** is able to produce a combined effect that results in the inhibition of HIF-1 activation and its target gene expression at the molecular level, suppression of tumor angiogenesis, metastasis, and tumor cell viability/proliferation at the cellular level. Proteins such as HIF-1α that have a short half-life may be exquisitely sensitive to inhibitors of protein synthesis. In our studies and those of others, protein synthesis inhibitors such as emetine suppress HIF-1 activation and the induction of downstream target genes (26, 27). Under hypoxic conditions, there is an overall decrease in protein synthesis. This may amplify the inhibitory effects exerted by protein synthesis inhibitors on the panel of proteins expressed under hypoxic conditions. Tumor cells are constantly mutating to adapt to their environment. By targeting multiple processes that are essential for tumor cells to adapt and survive, compounds such as **2** may offer an improved therapeutic outcome against tumors relative to the effects produced by a single target/process-specific agent. The relatively simple structure of **2** provides an attractive target for structural modification and pharmacological optimization.

Acknowledgments—We thank Dr. Steven L. McKnight (University of Texas Southwestern) for the pHRE-TK-luc construct, Dr. Stephen W. Morris (St. Jude Children's Research Hospital) for reviewing the manuscript, and the National Center for Natural Products Research (University of Mississippi) for the plant material.

REFERENCES

1. Harris, A. L. (2002) *Nat. Rev. Cancer* **2,** 38–47
2. Le, Q. T., Denko, N. C., and Giaccia, A. J. (2004) *Cancer Metastasis Rev.* **23,**

[4] Y.-D. Zhou and D. G. Nagle, unpublished observations.

293–310
3. Tatum, J. L., Kelloff, G. J., Gillies, R. J., Arbeit, J. M., Brown, J. M., Chao, K. S., Chapman, J. D., Eckelman, W. C., Fyles, A. W., Giaccia, A. J., Hill, R. P., Koch, C. J., Krishna, M. C., Krohn, K. A., Lewis, J. S., Mason, R. P., Melillo, G., Padhani, A. R., Powis, G., Rajendran, J. G., Reba, R., Robinson, S. P., Semenza, G. L., Swartz, H. M., Vaupel, P., Yang, D., Croft, B., Hoffman, J., Liu, G., Stone, H., and Sullivan, D. (2006) *Int. J. Radiat. Biol.* **82,** 699–757
4. Dewhirst, M. W. (1998) *Semin. Radiat. Oncol.* **8,** 143–150
5. Graeber, T. G., Osmanian, C., Jacks, T., Housman, D. E., Koch, C. J., Lowe, S. W., and Giaccia, A. J. (1996) *Nature* **379,** 88–91
6. Semenza, G. L., and Wang, G. L. (1992) *Mol. Cell. Biol.* **12,** 5447–5454
7. Wang, G. L., and Semenza, G. L. (1995) *J. Biol. Chem.* **270,** 1230–1237
8. Maxwell, P. H., Wiesener, M. S., Chang, G. W., Clifford, S. C., Vaux, E. C., Cockman, M. E., Wykoff, C. C., Pugh, C. W., Maher, E. R., and Ratcliffe, P. J. (1999) *Nature* **399,** 271–275
9. Ivan, M., Kondo, K., Yang, H., Kim, W., Valiando, J., Ohh, M., Salic, A., Asara, J. M., Lane, W. S., and Kaelin, W. G., Jr. (2001) *Science* **292,** 464–468
10. Jaakkola, P., Mole, D. R., Tian, Y. M., Wilson, M. I., GieIbert, J., Gaskell, S. J., Kriegsheim, A. V., Hebestreit, H. F., Mukherji, M., Schofield, C. J., Maxwell, P. H., Pugh, C. W., and Ratcliffe, P. J. (2001) *Science* **292,** 468–472
11. Lando, D., Peet, D. J., Whelan, D. A., Gorman, J. J., and Whitelaw, M. L. (2002) *Science* **295,** 858–861
12. Isaacs, J. S., Jung, Y. J., Mimnaugh, E. G., Martinez, A., Cuttitta, F., and Neckers, L. M. (2002) *J. Biol. Chem.* **277,** 29936–29944
13. Liu, Y. V., Baek, J. H., Zhang, H., Diez, R., Cole, R. N., and Semenza, G. L. (2007) *Mol. Cell* **25,** 207–217
14. Semenza, G. L. (2003) *Nat. Rev. Cancer* **3,** 721–732
15. Semenza, G. L. (2007) *Drug Discov. Today* **12,** 853–859
16. Zhong, H., de Marzo, A. M., Laughner, E., Lim, M., Hilton, D. A., Zagzag, D., Buechler, P., Isaacs, W. B., Semenza, G. L., and Simons, J. W. (1999) *Cancer Res.* **59,** 5830–5835
17. Birner, P., Schindl, M., Obermair, A., Plank, C., Breitenecker, G., and Oberhuber, G. (2000) *Cancer Res.* **60,** 4693–4696
18. Bos, R., Zhong, H., Hanrahan, C. F., Mommers, E. C., Semenza, G. L., Pinedo, H. M., Abeloff, M. D., Simons, J. W., van Diest, P. J., and van der Wall, E. (2001) *J. Natl. Cancer Inst.* **93,** 309–314
19. Ryan, H. E., Poloni, M., McNulty, W., Elson, D., Gassmann, M., Arbeit, J. M., and Johnson, R. S. (2000) *Cancer Res.* **60,** 4010–4015
20. Kung, A. L., Zabludoff, S. D., France, D. S., Freedman, S. J., Tanner, E. A., Vieira, A., Cornell-Kennon, S., Lee, J., Wang, B., Wang, J., Memmert, K., Naegeli, H. U., Petersen, F., Eck, M. J., Bair, K. W., Wood, A. W., and Livingston, D. M. (2004) *Cancer Cell* **6,** 33–43
21. Unruh, A., Ressel, A., Mohamed, H. G., Johnson, R. S., Nadrowitz, R., Richter, E., Katschinski, D. M., and Wenger, R. H. (2003) *Oncogene* **22,** 3213–3220
22. Moeller, B. J., Dreher, M. R., Rabbani, Z. N., Schroeder, T., Cao, Y., Li, C. Y., and Dewhirst, M. W. (2005) *Cancer Cell* **8,** 99–110
23. Rapisarda, A., Uranchimeg, B., Scudiero, D. A., Selby, M., Sausville, E. A., Shoemaker, R. H., and Melillo, G. (2002) *Cancer Res.* **62,** 4316–4324
24. Kong, D., Park, E. J., Stephen, A. G., Calvani, M., Cardellina, J. H., Monks, A., Fisher, R. J., Shoemaker, R. H., and Melillo, G. (2005) *Cancer Res.* **65,** 9047–9055
25. Tan, C., de Noronha, R. G., Roecker, A. J., Pyrzynska, B., Khwaja, F., Zhang, Z., Zhang, H., Teng, Q., Nicholson, A. C., and Giannakakou, P. (2005) *Cancer Res.* **65,** 605–612
26. Zhou, Y.-D., Kim, Y.-P., Mohammed, K. A., Jones, D. K., Muhammad, I., Dunbar, D. C., and Nagle, D. G. (2005) *J. Nat. Prod.* (*Lloydia*) **68,** 947–950
27. Chau, N. M., Rogers, P., Aherne, W., Carroll, V., Collins, I., McDonald, E., Workman, P., and Ashcroft, M. (2005) *Cancer Res.* **65,** 4918–4928
28. Jones, D. T., and Harris, A. L. (2006) *Mol. Cancer Ther.* **5,** 2193–2202
29. Hodges, T. W., Hossain, C. F., Kim, Y. P., Zhou, Y. D., and Nagle, D. G. (2004) *J. Nat. Prod.* (*Lloydia*) **67,** 767–771
30. Hossain, C. F., Kim, Y. P., Baerson, S. R., Zhang, L., Bruick, R. K., Mohammed, K. A., Agarwal, A. K., Nagle, D. G., and Zhou, Y. D. (2005) *Biochem. Biophys. Res. Commun.* **333,** 1026–1033
31. Jackson, B., Owen, P. J., and Scheinmann, F. (1971) *J. Chem. Soc. Perkin Trans. I* **20,** 3389–3392
32. Chandel, N. S., Maltepe, E., Goldwasser, E., Mathieu, C. E., Simon, M. C., and Schumacker, P. T. (1998) *Proc. Natl. Acad. Sci. U. S. A.* **95,** 11715–11720
33. Liao, D., Corle, C., Seagroves, T. N., and Johnson, R. S. (2007) *Cancer Res.* **67,** 563–572
34. Nagle, D. G., and Zhou, Y. D. (2006) *Curr. Drug Targets* **7,** 355–369
35. Newman, D. J., and Cragg, G. M. (2007) *J. Nat. Prod.* (*Lloydia*) **70,** 461–477
36. Fang, N., and Casida, J. E. (1999) *J. Agric. Food Chem.* **47,** 2130–2136
37. Vaux, E. C., Metzen, E., Yeates, K. M., and Ratcliffe, P. J. (2001) *Blood* **98,** 296–302
38. Han, X. H., Hong, S. S., Hwang, J. S., Jeong, S. H., Hwang, J. H., Lee, M. H., Lee, M. K., Lee, D., Ro, J. S., and Hwang, B. Y. (2005) *Arch. Pharm. Res.* (*Seoul*) **28,** 1324–1327
39. Na, M., Jang, J., Njamen, D., Mbafor, J. T., Fomum, Z. T., Kim, B. Y., Oh, W. K., and Ahn, J. S. (2006) *J. Nat. Prod.* (*Lloydia*) **69,** 1572–1576
40. Kingsford-Adaboh, R., Dittrich, B., Hübschle, C. B., Gbewonyo, W. S., Okamoto, H., Kimura, M., and Ishida, H. (2006) *Acta Crystallogr. Sect. B* **62,** 843–849
41. Bell, E. L., Klimova, T. A., Eisenbart, J., Moraes, C. T., Murphy, M. P., Budinger, G. R. S., and Chandel, N. S. (2007) *J. Cell Biol.* **177,** 1029–1036
42. Simon, M. C. (2006) *Adv. Exp. Med. Biol.* **588,** 165–170
43. Pan, Y., Mansfield, K. D., Bertozzi, C. C., Rudenko, V., Chan, D. A., Giaccia, A. J., and Simon, M. C. (2007) *Mol. Cell. Biol.* **27,** 912–925
44. Schroedl, C., McClintock, D. S., Budinger, G. R., and Chandel, N. S. (2002) *Am. J. Physiol.* **283,** L922–L931
45. Gong, Y., and Agani, F. H. (2005) *Am. J. Physiol.* **288,** C1023–C1029
46. Guzy, R. D., Hoyos, B., Robin, E., Chen, H., Liu, L., Mansfield, K. D., Simon, M. C., Hammerling, U., and Schumacker, P. T. (2005) *Cell Metab.* **1,** 401–408
47. Lin, X., David, C. A., Donnelly, J. B., Michaelides, M., Chandel, N. S., Huang, X., Warrior, U., Weinberg, F., Tormos, K. V., Fesik, S. W., and Shen, Y. (2008) *Proc. Natl. Acad. Sci. U. S. A.* **105,** 174–179
48. Rucci, N., Susa, M., and Teti, A. (2008) *Anticancer Agents Med. Chem.* **8,** 342–349
49. Wang, G. L., Jiang, B. H., and Semenza, G. L. (1995) *Biochem. Biophys. Res. Commun.* **216,** 669–675
50. Richard, D. E., Berra, E., Gothie, E., Roux, D., and Pouyssegur, J. (1999) *J. Biol. Chem.* **274,** 32631–32637